Environ. Sci. Technol. **2010,** *44,* 9213–9218

Viability and Metal Reduction of *Shewanella oneidensis* MR-1 under CO_2 Stress: Implications for Ecological Effects of CO_2 Leakage from Geologic CO_2 Sequestration

BING WU, HONGBO SHAO, ZHIPENG WANG, YANDI HU, YINJIE J. TANG, AND YOUNG-SHIN JUN*

Department of Energy, Environmental and Chemical Engineering, Washington University, St. Louis, Missouri 63130, United States

Received July 8, 2010. Revised manuscript received October 19, 2010. Accepted October 21, 2010.

To study potential ecological impacts of CO_2 leakage to shallow groundwater and soil/sediments from geologic CO_2 sequestration (GCS) sites, this work investigated the viability and metal reduction of *Shewanella oneidensis* MR-1 under CO_2 stress. While MR-1 could grow under high-pressure nitrogen gas (500 psi), the mix of 1% CO_2 with N_2 at total pressures of 15 or 150 psi significantly suppressed the growth of MR-1, compared to the N_2 control. When CO_2 partial pressures were over 15 psi, the growth of MR-1 stopped. The reduced bacterial viability was consistent with the pH decrease and cellular membrane damage under high pressure CO_2. After exposure to 150 psi CO_2 for 5 h, no viable cells survived, the cellular contents were released, and microscopy images confirmed significant cell structure deformation. However, after a relatively short exposure (25 min) to 150 psi CO_2, MR-1 could fully recover their growth within 24 h after the stress was removed, and the reduction of MnO_2 by MR-1 was observed right after the stress was removed. Furthermore, MR-1 survived better if the cells were aggregated rather than suspended, or if pH buffering minerals, such as calcite, were present. To predict the cell viability under different CO_2 pressures and exposure times, a two-parameter mathematical model was developed.

1. Introduction

The amount of carbon dioxide (CO_2) from anthropogenic emissions has dramatically increased in the past several decades, which raises global climate-change concerns. CO_2 sequestration in deep geological formations (i.e., geologic CO_2 sequestration, GCS), such as deep saline aquifers, provides a promising option for us to significantly reduce net CO_2 emissions to the atmosphere within a relatively short period (Figure 1) (*1*−*3*). For successful geologic CO_2 sequestration, the injected CO_2 should remain stable in the GCS sites. However, zero leakage of CO_2 from GCS projects may not be possible. Analog studies of geologic environments containing large, concentrated amounts of CO_2 have shown that the leakage processes is inherent in GCS (*4*). Leaking of CO_2 could be due to the presence of preexisting geological discontinuities, the weakening of the caprock caused by interactions with CO_2, or incidental breakouts through injection wells, existing wells, or seismic disturbances (*1*). It has been estimated that allowing for no more than 1% leakage of stored CO_2 over 100 years is necessary for sequestration to be viable (*5*). Once any leakage from deep geological formations occurs, CO_2 can migrate through overlying potable aquifers and induce geological, chemical, and/or microbiological changes in shallow groundwater, which can be an underground source of drinking water (USDW), and in soil/sediment environments (Figure 1) (*1, 3, 6*−*8*). Dissolved in groundwater, CO_2 increases the total concentration of aqueous carbonate species, including H_2CO_3, HCO_3^-, and CO_3^{2-}, and causes a decrease in pH. Such conditions can also influence the viability and activity of microorganisms, while changing the reaction mechanisms of dissolution, adsorption (*8*), precipitation, and redox reactions occurring on mineral surfaces or in the aqueous phase. Systematic studies of potential impacts of CO_2 leakage on biogeochemistry and ecosystems are required to ensure safer GCS.

Shewanella species are environmentally relevant bacteria, widely existing in soil and sediments (*9*), where CO_2 leaking from sequestration sites may pass through (Figure 1). *S. oneidensis* MR-1 is a model *Shewanella* strain and can grow in both aerobic and anaerobic environments (convenient for laboratory handling) due to its facultative anaerobic characteristics. In this study, *S. oneidensis* MR-1 is selected as a model microorganism to study the effect of CO_2 leakage on the subsurface ecological system. In particular, the metal reducing capability of *S. oneidensis* MR-1, such as Fe(III), Mn(IV), and Cr(VI) in soil/sediment environments (*10*−*14*), is an important aspect which can affect toxic metal mobility in the environment. Therefore, by examining *S. oneidensis* MR-1 physiology, the following crucial information can be obtained: (1) aerobic and anaerobic microorganism survival and recovery in response to various CO_2 conditions and (2) the impacts of higher CO_2 concentrations owing to potential leakage on intrinsic microbial activities (e.g., metal reduction) and water chemistry changes in groundwater above GCS sites. Currently, a few studies have focused on utilizing biofilms to prevent CO_2 migration to upper geological matrices (*15, 16*) or on enhancing mineral-trapping and solubility-trapping though microbial ureolysis (*17*). These approaches decrease the porosity and permeability of the caprock, potentially alleviating CO_2 leakage. However, little is known about the ecological impacts near GCS sites of exposure to high pressure CO_2.

To understand the influence of CO_2 leakage on microbial activity, we measured the changes in viability and metal reduction rates of MR-1 after exposure to increased CO_2 concentrations. Reduction rates of MnO_2 were used to evaluate the activity of MR-1 for three reasons: first, MnO_2 is widely distributed in the natural environment (*18*). Second, it is one of the primary electron acceptors for organic matter oxidation and plays an important role in carbon mineralization in sedimentary environments (*11*). Third, MnO_2 reduction by MR-1 is a relatively fast reaction (*10, 11, 14*), which allows us to evaluate the activity of stressed MR-1 before it is recovered. We also examined bacterial responses to CO_2 stress in the presence of calcite coupons by combining biological and physicochemical approaches. A mathematical model was built to quantitatively demonstrate and predict CO_2 stress on microbial survival in the ecological system. This study can help us understand the potential ecological effects of high-pressure CO_2 and provide guidelines to control CO_2 leakage from the GCS sites.

* Corresponding phone: (314)935-4539; fax: (314)935-7211; e-mail: ysjun@seas.wustl.edu;http://encl.engineering.wustl.edu/.

10.1021/es102299j © 2010 American Chemical Society
Published on Web 11/08/2010

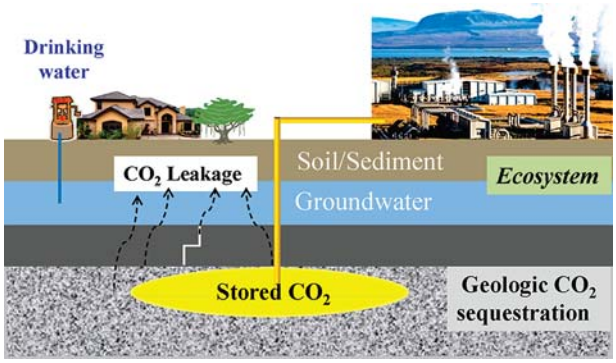

FIGURE 1. Schematic diagram of potential scenario for ecological and environmental impact of CO_2 leakage from geologic CO_2 sequestration sires.

2. Materials and Methods

2.1. Reactor Setup and Experimental Conditions. In this work, a bioreactor (Parr company, USA) was used to mimic the exposure of bacteria in groundwater to CO_2 leakage from GCS sites. This reactor was combined with a syringe pump connected to a CO_2 cylinder (99.9%, Airgas, USA) as a source for pressurized CO_2 (For more detailed information, refer to Figure S1 and ref *19*.). Before the experiments, the reactor was flushed with CO_2 and/or N_2 (in some experiments) for two minutes to remove the air in the reactor. After that, the reactor was pressurized to the designated pressure through the syringe pump and pump controller. In this reactor setup, a temperature controller system maintained the reactor at a constant temperature (32 ± 0.5 °C). CO_2 and N_2, singly or in mixtures, were used at a variety of pressures: 1% CO_2/99% N_2 (0.15 psi CO_2 in a total of 15 psi), 1% CO_2/99% N_2 (1.5 psi CO_2 in a total of 150 psi), 100% CO_2 (15 psi), 100% CO_2 (80 psi), and 100% CO_2 (150 psi). This tested CO_2 range covered the concentrations typically present either in flue gas from a conventional power station (*20*) or in groundwater (*8*).

2.2. Microorganism Cultivation. *Shewanella oneidensis* MR-1 was first grown in a Luria−Bertani (LB) medium at 32 ± 0.5 °C. The bacteria were then subcultured into an MR-1 medium (30 mM lactate as the carbon source) (*14*). When MR-1 growth reached the middle log phase (optical density (OD) measured at 600 nm was about 0.7), a second subculture (5% inoculation rate) was transferred into a modified MR-1 medium which supported anaerobic growth. The modified medium was supplemented with 40 mM fumarate (Sigma, USA) as an electron acceptor and with 0.5 mM serine and 0.5 mM glycine (Sigma, USA) as nutrients to enhance cell growth (*14*). Falcon test tubes with 4 mL of the cell culture (initial OD_{600} ~ 0.2) were placed in the reactor for CO_2 exposure experiments. Control samples (without CO_2 stress) were cultured in sealed bottles (i.e., in a microaerobic condition). All culture experiments with CO_2 (including control samples) were kept at 32 ± 0.5 °C without shaking.

For CO_2 stress experiments, the cultures with or without calcite coupons were exposed to high pressure CO_2 in the reactor for a designated time. We added calcite coupons (0.12 g/mL; Iceland spar from New Mexico) to test the response of bacteria to CO_2 stress in the presence of pH buffering minerals. After CO_2 exposure, the total number of viable cells was estimated based on the number of colony-forming unit (CFU) after incubation at 32 ± 0.5 °C for 1−2 days. Averaged values and errors (standard deviations) of multiple samples (biological repeat, $n \geq 4$) are presented in the figures. The statistical significance of the mean values was examined by one-way analysis of variance at $p < 0.05$. To observe bacterial growth recovery after exposure to CO_2, the stressed cells (1 mL) were transferred into a tube filled with 5 mL of MR-1 minimal media and cultured in the incubator under aerobic conditions at 32 ± 0.5 °C. To examine the MR-1 cell aggregates under CO_2 stress, the cultures were filtered through a membrane (~1 cm × 1 cm, 0.22 μm pore size, Nylon, Millipore, USA) to form loosely attached cell layers (cell density was ~8.0 × 10^{10} cells/m^2) and then were transferred to the reactor for stress experiments.

2.3. Measurement of Extracellular Polymeric Substances (EPS) and Membrane Integrity. In this study, the concentrations of EPS, including DNA, polysaccharides, and proteins, were analyzed. For EPS concentration, a modified EPS extraction method was utilized to quantify the EPS during experiments (*21*). The concentrations of polysaccharides and proteins were analyzed according to methods described by Dubois et al. (*22*) and Bradford (*23*), respectively. The integrity of the cytoplasmic membrane of cells was determined using a BacLight Live/Dead Kit (Molecular Probes, Invitrogen, USA). More detailed experimental descriptions are available in the Supporting Information. For all the measurements, three biological repeats and two technical repeats were conducted.

2.4. Scanning Electron Microscopy (SEM) and Atomic Force Microscopy (AFM) Observations of Microbial Cells. For SEM sample preparation, the cells were deposited on a piece of membrane and then were fixed by adding 2% glutaraldehyde. After 2 h, the samples were washed three times in 0.10 M sodium cacodylate buffer for 20 min each time. The samples were then dehydrated in a series of 10 min washes in 50%, 70%, 85%, and 95% ethanol and were further dried with freeze-drier equipment (Labconco, USA). This procedure allowed us to maintain the cell morphology during SEM measurements (*24*). The samples were gold-coated using a sputter gun (SPI supplies, USA). Photographs of the sample structure were observed and taken with a SEM (FEI, UK).

For AFM observation of cells, the cells were deposited on a quartz coupon (~1 cm × 1 cm) in the presence of aqueous media. The heights, deflection, and friction images of the samples were collected simultaneously in contact mode using a Nanoscope V Multimode SPM (Veeco Instruments Inc., USA). Due to the strong stickiness of the released cell materials, the AFM observations were mainly focused on the cell morphology rather than the observation of released cell materials. Probes were made of nonconductive silicon nitride, with a tip height of 196 μm (NP-S10, Veecoprobes, USA). The images were collected with normal spring constants of 0.12 N/m and scan rates of around 1.5 Hz. Topographical features were analyzed using Nanoscope software (Version 7.20, Veeco Instruments Inc., USA).

2.5. Measurements of Ca^{2+} Release from Calcite Coupons, Lactate Consumption. Cell cultures (OD_{600} ~ 0.25, viable cells ~ 10^8/mL) were added to two sterile bottles (20 mL). The same number of freshly cleaved calcite coupons was added in the same liquid/solid ratio as in all experiments conducted in the reactor. Both bottles were tightly covered with Parafilm laboratory film, and 100% CO_2 (15 psi) was introduced from a CO_2 cylinder (Airgas, USA) through pipelines to the headspaces of the bottles. The pH changes were monitored using a pH meter (Orion, Thermo Scientific, USA). Samples were collected at designated times (1, 5, and 17 h) with syringes and were used to measure CFU and the concentrations of calcium ions (Ca^{2+}) and lactate. The calcium was measured with an inductively coupled plasma mass spectrometer (ICP-MS, Agilent, USA). Because lactate was the main carbon source for MR-1 growth, the consumption of lactate during the high CO_2 stress conditions was also determined by a lactate assay kit (R-Biopharm, Germany) (*14*).

2.6. MnO_2 Reduction Capability Measurements. Manganese reduction by stressed and unstressed cells was measured. The cells were exposed to 100% CO_2 under 150 and 300 psi in the reactor at 32 ± 0.5 °C (stressed cells) or were cultured in an incubator at 32 ± 0.5 °C (nonstressed

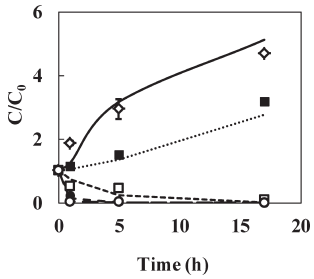

FIGURE 2. The measured growth and modeled growth of *S. oneidensis* MR-1 under CO_2 stress ($n \geq 4$): (◇) 1% CO_2 (15 psi); (■) 1% CO_2 (150 psi); (□) 100% CO_2 (15 psi); (•) 100% CO_2 (80 psi); (○) 100% CO_2 (150 psi). The error bars are smaller than the symbols, and here unseen. The lines are the predicted curves based on fitting the data to eq 2 and eq 3: (solid) 1% CO_2 (15 psi); (round dot) 1% CO_2 (150 psi); (square dot) 100% CO_2 (15 psi); (dash) 100% CO_2 (80 psi); (long dash) 100% CO_2 (150 psi). C/C_0 is the ratio of the viable cells number after CO_2 stress to the initial cell number.

cells). Under both conditions, fumarate was not added into the medium because it can compete with MnO_2 for electrons. After 25 min, 30 mL of stressed or nonstressed cell cultures was placed in serum bottles and deoxygenated by sparging with nitrogen (atmosphere pressure) for 15 min (to achieve anaerobic conditions). Then 1 g of MnO_2 (Sigma-Aldrich, purity >99%) was added to each serum bottle, and nitrogen sparging was continued for another 3 min before the serum bottles were crimp sealed with Teflon-lined stoppers and aluminum seals. Then the bottles were placed on a rotating shaker (40 rotations per min) in an incubator at 32 ± 0.5 °C in the dark (time t_0). At the desired time points, an aliquot of the suspension (including both the well-mixed liquid and solid) was withdrawn through the septum with a N_2 purged gastight syringe. Part of the suspension was used for CFU analysis, and the remainder was passed though a 0.22 μm filter and diluted with 2% HNO_3 solution for manganese measurement with ICP-MS. The reaction rates of MnO_2 were calculated from the data within the first 40 min by linear regression ($R^2 > 0.98$).

3. Results and Discussion

3.1. Cell Viability under CO_2 Stress. The growth and viability of MR-1 were strongly affected by both CO_2 partial pressure and exposure time. Figure 2 shows the viable cells after MR-1 was exposed to CO_2 under partial pressures ranging from 0.15 to 150 psi. Under low CO_2 partial pressures (i.e., 0.15 and 1.5 psi, equivalent to 1% CO_2 when the pressures were 15 and 150 psi, respectively), the cell growth appeared to be inhibited. When the CO_2 pressure approached 15 psi (100% CO_2), the cell growth was completely stopped, and the viable cell numbers decreased as a function of exposure time. Increasing CO_2 pressure to 80 and 150 psi (100% CO_2) resulted in a dramatic drop of viable cells within 1 h, and no viable cells were detected after 5 h. For the experiment conducted at 150 psi (100% CO_2) for 1 h, the OD values were also measured. The results showed that the OD values remained constant before or after CO_2 exposure, while the CFU value decreased by approximately 2 orders of magnitude. This suggests that only a small portion of cells remain viable, and the majority of cells were damaged or died.

CO_2 gas may affect microbial activity through three routes: high pressure stress on cellular structures, altered environmental pH from CO_2 dissolution, and CO_2 penetration intracellularly to interfere with metabolic functions. N_2 gas was employed to study the effect of pressure alone on bacterial viability. At N_2 gas pressures of 500 psi, bacterial growth was only slightly suppressed by about 13.0 ± 0.5% during a 17 h period (data not shown). Also, an experiment with a sudden influx of 100% CO_2 at 150 psi, followed by its immediate release (within 5 s, *in situ* pH changed merely about 0.01 (Figure S2)) did not lead to any obvious influence on bacterial viability (similar CFU counts were detected; data not shown). Both phenomena indicate that pressure itself appeared not to be the key influence on microbial viability. Further, we examined pH conditions during CO_2 stress (atmosphere pressure). When 1.5 psi CO_2 was introduced into the bioreactor, the *in situ* pH in the medium was 6.16 after 1 h exposure (Figure S2), and the viable cells were maintained at 59.1 ± 7.4% of the initial subcultures. In comparison, a culture with pH = 6.16 (adjusted by 0.2 M HCl, without CO_2 stress) did not result in any obvious changes in bacterial viability within 1 h (viable cells were kept at 100.0 ± 8.6%). At 150 psi CO_2 for 1 h, the pH in the culture dropped to 4.86, and the viable cell amounts were about 0.7 ± 0.1%. However, the culture with the same pH (pH only adjusted by HCl) without CO_2 stress had a cellular viability of 23.2 ± 14.7%.

The above results indicate that besides the pH effect, CO_2 put significant stresses on cells. High pressure CO_2 can diffuse through cell membranes and dissolve intracellularly because of the hydrophobic and liposoluble properties of the cellular membrane. This process may increase membrane permeability, destroy the integrity of the cellular structure, and change the intracellular metabolic balance (*25−27*). This explanation was supported by the following observations: after exposure of cells to CO_2 (100%, 150 psi) for 1 h, a significant amount of extracellular protein (619 ± 31 mg/g of dry biomass) was released, whereas for unstressed cells, the value was only 282 ± 14 mg/g. The increase in extracellular protein for stressed cells was accompanied by an increase of free DNA concentration in the solution, from 17.8 ± 0.3 ng/μL for unstressed cells to 27.4 ± 2.2 ng/μL. Furthermore, a decrease of membrane integrity index from 2.05 ± 0.18 for unstressed cells to 0.39 ± 0.06 for stressed cells was observed (Table S1). SEM images (Figure 3-A, B, and C) show the morphological changes of cells with progressively longer CO_2 exposure times. AFM images (Figures 3-D, E, and F) also indicate that the unstressed cell thickness was 207 ± 42 nm, with a cell length ranging around 2.02 ± 0.32 μm (Figure 3-D, profile-i). After exposure to CO_2 (150 psi) for 30 min and 5 h, respectively, the thicknesses of the cells were reduced to 102 ± 32 nm (Figure 3-E, profile-ii) and 49 ± 11 nm (Figure 3-F, profile-iii), respectively. The cell lengths were reduced to 1.60 ± 0.28 μm and 1.72 ± 0.32 μm (the values above are based on the measurement for 20 cells, and the uncertainties are standard deviations). These results confirmed that a large number of cells were collapsed, and thus cellular contents (such as protein and nucleotides) were released.

3.2. Alleviation of CO_2 Stress under Environmental Conditions. Previous studies have reported that bacterial aggregates and biofilms could be considered as cellular response mechanisms to tolerate high CO_2 stress (*15, 16*). In this study, loosely attached microbial cell aggregates were developed by directly filtrating cells on a membrane (yielding a cell density of ~8.0×10^{10} cells/m^2) and then exposing them to 100% CO_2 at 150 psi for 30 min. More viable cells (by 1−2 orders of magnitude) were achieved for aggregated cells than in the suspended culture (Table S1). This observation was consistent with findings in the literature that microbial cell aggregation can limit mass transport and create a microenvironment for cells to resist environmental stresses (such as pH and oxygen stress) (*10, 15, 16*). Furthermore, when the stressed cells (100% CO_2 at 150 psi for 25 min) were transferred into a normal culture medium, their growth rate (defined by the change of OD values in an hour of bacterial growth) in the exponential phase was about 0.08 h^{-1}, which was clearly lower than that of unstressed cells (with a growth rate of 0.32 h^{-1}) (Figure S3B). However, the stressed cells

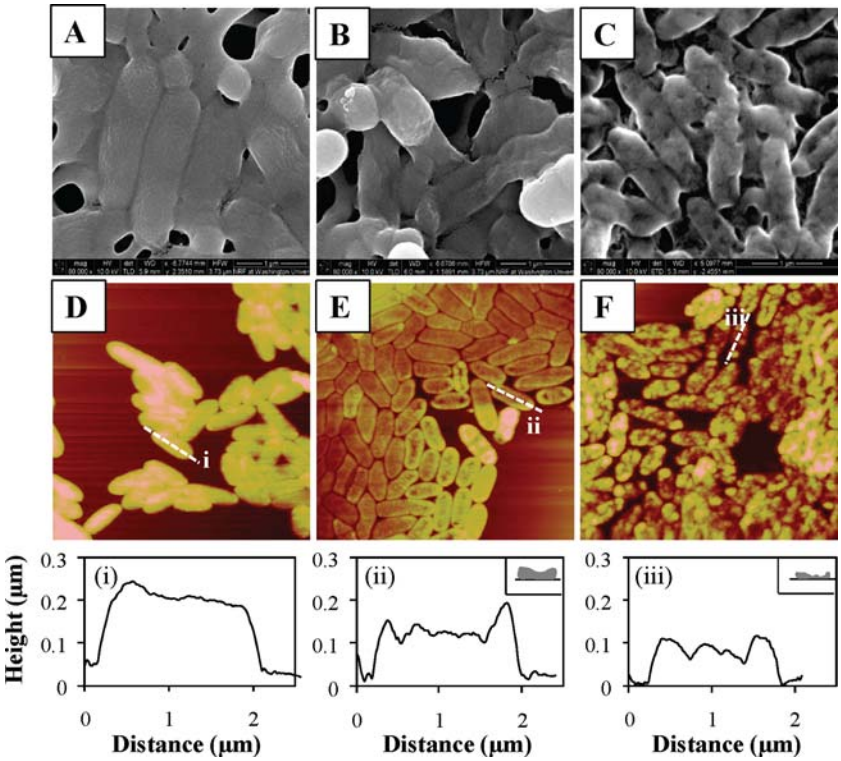

FIGURE 3. SEM and AFM images of *S. oneidensis* cells before and after CO_2 stress (100% CO_2, 150 psi): (A) and (D) unstressed cells; (B) and (E) cells after CO_2 stress for 30 min; (C) and (F) cells after CO_2 stress for 5 h. (A), (B), and (C) are SEM images and (D), (E), and (F) are AFM images. The AFM micrograph is shown in height mode (15 × 15 μm^2) at 298 K in air in the presence of aqueous media on quartz coupon surfaces. The height cross sections correspond to the white dotted lines in the AFM images.

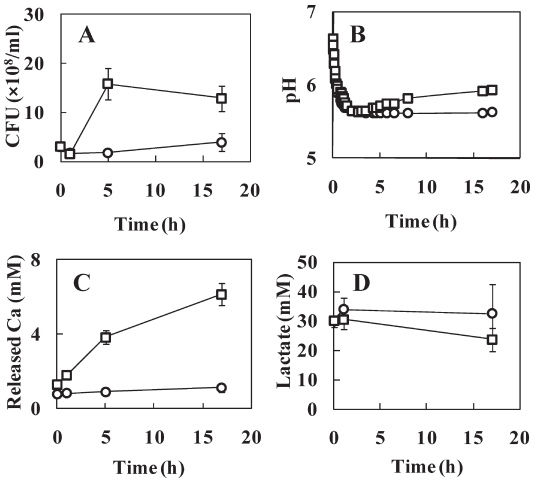

FIGURE 4. Changes of (A) CFU, (B) *in situ* pH values, (C) calcium concentrations, and (D) lactate concentrations in the presence of calcite coupons under CO_2 stress (100% CO_2, 15 psi) ($n \geq 3$): (○) control cells and (□) cells in the presence of calcite coupons. The error bars are smaller than the symbols and here unseen.

could recover to the same cell density as the unstressed cells within 24 h after a long lag phase, which indicates that MR-1 displayed excellent recovery ability once the CO_2 stresses are removed.

The effect of calcite coupons on alleviating CO_2 stress to the cells was tested because calcite can serve as a pH buffering mineral in the presence of high pressure CO_2 (*8*). Figure 4A shows 3-fold viable cells were achieved after adding calcite coupons, compared to the number without calcite coupons. This finding corresponds to the fact that adding calcite coupons into the medium could lead to an increase of *in situ* pH by about 0.3 unit, after an equilibration process for 3 h (Figure 4B). Figure 4C suggests that calcite coupons gradually released Ca^{2+} in the solution (this concentration of Ca^{2+} could not directly inhibit the growth of MR-1). Calcite dissolution can, however, neutralize the acidic solutions resulting from the dissolved CO_2 and thus reduce pH stress on microbial cells. In addition, utilization of lactate could cause pH decrease in the culture solution. However, we did not observe a significant change of lactate concentrations in the absence or the presence of calcite coupons within 17 h (Figure 4D).

3.3. MnO_2 Reduction by Stressed Cells. Under anaerobic conditions, MR-1 can use Mn(IV) as an electron acceptor and reduce Mn(IV) (i.e., MnO_2) to Mn(II), which becomes aqueous Mn^{2+} (*11*). In this study, the metabolic function of the stressed MR-1 was evaluated by monitoring the reaction rate of Mn(II) formation when MnO_2 was present in the MR-1 cultures. The results suggest that MnO_2 dissolution or reduction in the medium (without cells) was negligible (Figure 5). For the unstressed cells, the aqueous Mn concentration increased linearly with time in the early reaction period and arrived at the maximum value after 1.5 h (Figure 5). The stressed cells were also observed to have a capability to reduce Mn(IV), although their reduction rates (4.74 ± 0.25 and 1.66 ± 0.17 μmol/h under CO_2 of 150 and 300 psi, respectively) were significantly lower than that of unstressed cells (8.33 ± 0.16 μmol/h) (Figure 5B). These results indicated that CO_2 stress did not influence the metabolic function of MR-1: the stressed cells could reduce Mn(IV) immediately after the stress was removed.

3.4. Modeling Bacterial Viability under CO_2 Stress. To prudently explain the complex influence of high pressure CO_2 on bacterial survival in a dose-time dependent manner, a simple mathematical model was built using the first order growth and decay model given in eq 1

$$\frac{dC}{dt} = k_1 C - k_2 C P_{CO_2} \quad (1)$$

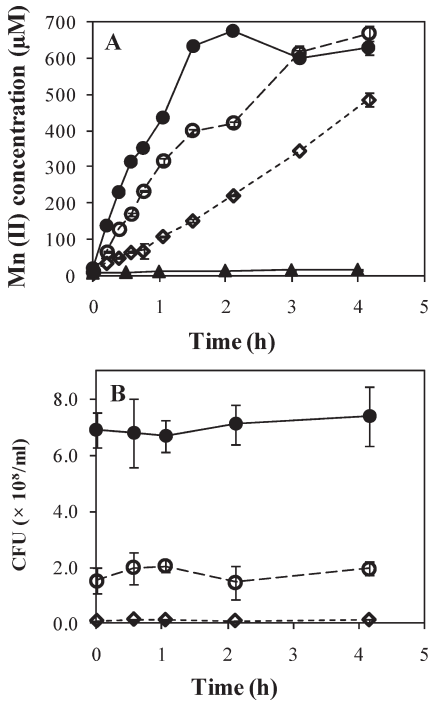

FIGURE 5. Mn(II) concentration (A) and CFU (B) during MnO_2 reduction by CO_2 stressed and nonstressed cell: (▲) control experiment without cells; (•) control experiment with unstressed cells; (○) stressed cells under 100% CO_2, 150 psi for 25 min; (◇) stressed cells under 100% CO_2, 300 psi for 25 min. The error bars are smaller than the symbols and here unseen.

where C is the viable bacterial cell numbers at time t, k_1 is the specific growth rate (h^{-1}), k_2 is the specific death rate constant (psi^{-1} h^{-1}) under CO_2 stress, and P_{CO_2} (psi) is the partial pressure of CO_2. k_1C describes normal growth without any limiting factors, which follows a simple exponential curve. $k_2CP_{CO_2}$ represents bacterial death, which is limited by the partial pressure of CO_2.

Integrating eq 1 with the initial conditions as $t = 0$ and $C = C_0$

$$\frac{C}{C_0} = \exp(k_1 t - k_2 t P_{CO_2}) \quad (2)$$

For partial pressures of $CO_2 \leq 0.15$ psi and time periods of CO_2 stress ≤ 5 h (solid line in Figure 2), $k_2P_{CO_2} \ll k_1$; thus eq 2 reduces to eq 3

$$\frac{C}{C_0} = \exp(k_1^* t) \quad (3)$$

Monte Carlo simulation provided by MATLAB (MathWorks, USA) was employed to generate 50 equal-sized data sets for C, and a genetic algorithm was used to fit the model parameters of k_1, k_1*, and k_2 with each simulated data set. According to the experimental data, the growth rates k_1 and k_1*, and the death rate k_2, were calculated to be about 0.12 ± 0.02, 0.23 ± 0.02, and 0.027 ± 0.007, respectively.

The calculated C/C_0 values using the parameters (k_1 = 0.12, $k_1^* = 0.23$, and $k_2 = 0.027$) are plotted as a function of time in Figure 2. The assessment on the goodness of the model fit was tested based on the minimization of the error between the fitting data and measured data. When the error was the minimal, the fitting data were considered optimal. The measured C/C_0 data from the above experiments fit well with the calculated values (Figure 2), which validated the model's ability to predict the effect of CO_2 on microbial survival.

4. Environmental Implications

The potential impacts of CO_2 leakage from geologic sequestration sites on surrounding geological properties and ecological systems are complicated and diverse. For example, CO_2 leakage might not uniformly distribute throughout the GCS site, and bacterial communities could exhibit different responses to CO_2 stress. This study simplifies the situation by employing an environmentally relevant bacterium (*S. oneidensis* MR-1) to represent the microbial ecosystem in response to CO_2 stress.

According to a previous study on the Frio geologic carbon sequestration test site, with 10% leakage of injected CO_2, the pH of groundwater can change from 6.7 to 5.3 within 20 m from the leak point (*28*). This pH change is very similar to that observed in our system. It has been reported that MR-1 can survive in a broad range of fluctuating pH (between 4 and 10 under aerobic conditions and from 5.6 to 9.4 under oxygen-limited conditions) (*10, 29*). This study shows that high pressure CO_2 may damage cells more than the pH effect. In addition, we observed that MR-1 cell growth resumed its normal rate after CO_2 exposure was stopped. Further, the stressed MR-1 displayed the MnO_2 reduction capability, although the reduction rate was lower. This implies that such a level of CO_2 leakage may not significantly influence the self-cleaning capability of groundwater near a GCS site, especially once the stress is removed. Also in soil/sediment systems, bacteria tend to attach on the minerals in the form of biofilm, and the presence of pH buffering minerals, such as calcite and other metal carbonates, could protect microbial ecology systems against CO_2 stress. However, the released metal species may also affect groundwater quality and soil/sediment composition by reacting with minerals in the presence of leaking CO_2. These reactions merit further study. This study provides fundamental information for an understanding of the impact of CO_2 leakage on microbial survival and metal reduction activity. These findings may affect the ecosystems as well as underground sources of drinking water and also help design a more accurate predictive model of the ecological impacts of leakage.

Acknowledgments

B.W. and H.S. contributed equally to this project. This study was partly supported by grants to Jun lab and Tang lab from the International Center for Advanced Renewable Energy and Sustainability (I-CARES) and The Consortium for Clean Coal Utilization at Washington University. Also, Y.S.J. and Y.H. were partly supported by the U.S. Department of Energy, in association with the Energy Research Frontier Center (EFRC) of Berkeley Lab (under Contract No. DE-AC02-05CH11231). We would like to thank the Nano Research Facility (NRF) at Washington University for the use of SEM.

Supporting Information Available

A description of the experimental procedures, one table, and three figures. This material is available free of charge via the Internet at http://pubs.acs.org.

Literature Cited

(1) Bruant, R. G.; Guswa, A. J.; Celia, M. A.; Peters, C. A. Safe storage of CO_2 in deep saline aquifers. *Environ. Sci. Technol.* **2002**, *36* (11), 240–245.

(2) Burruss, R. C.; Brennan, S. T.; Freeman, P. A.; Merrill, M. D.; Ruppert, L. F.; Becker, M. F.; Herkelrath, W. N.; Kharaka, Y. K.; Neuzil, C. E.; Swanson, S. M.; Cook, T. A.; Klett, T. R.; Nelson, P. H.; Schenk, C. J. Development of a Probabilistic Assessment Methodology for Evaluation of Carbon Dioxide Storage: U.S. Geological Survey Open-file 2009-1035, In 2009; . 81p. Available only online at http://pubs.usgs.gov/of/2009/1035/ (accessed June 30, 2010).

(3) Nordbotten, J. M.; Celia, M. A.; Bachu, S.; Dahle, H. K. Semianalytical solution for CO_2 leakage through an abandoned well. *Environ. Sci. Technol.* **2005**, *39* (2), 602–611.
(4) Nelson, C. R.; Evans, J. M.; Sorensen, J. A.; Steadman, E. N. Factors affecting the potential for CO_2 leakage from geologic sinks, Plain CO_2 reduction (PCOR) Partnership, 2005. Available only online at http://www.undeerc.org/PCOR/newsandpubs/pdf/FactorsAffectingPotential.pdf (accessed June 30, 2010).
(5) DOE Carbon Sequestration Technology Roadmap and Program Plan. U.S. DOE and NETL: Washington DC, 2007.
(6) Chang, K. W.; Minkoff, S. E.; Bryant, S. L. Simplified Model for CO_2 Leakage and its Attenuation due to Geological Structures. *Energy Procedia* **2009**, *1*, 3453–3460.
(7) Kutchko, B. G.; Strazisar, B. R.; Lowry, G. V.; Dzombak, D. A.; Thaulow, N. Rate of CO_2 attack on hydrated Class H well cement under geologic sequestration conditions. *Environ. Sci. Technol.* **2008**, *42* (16), 6237–6242.
(8) Wang, S.; Jaffe, P. R. Dissolution of a mineral phase in potable aquifers due to CO_2 releases from deep formations; effect of dissolution kinetics. *Energy Convers. Manage.* **2004**, *45* (18−19), 2833–2848.
(9) Hau, H. H.; Gralnick, J. A. Ecology and Biotechnology of the Genus Shewanella. *Annu. Rev. Microbiol.* **2007**, *61* (1), 237–258.
(10) Tang, Y. J. J.; Laidlaw, D.; Gani, K.; Keasling, J. D. Evaluation of the effects of various culture conditions on Cr(VI) reduction by Shewanella oneidensis MR-1 in a novel high-throughput mini-bioreactor. *Biotechnol. Bioeng.* **2006**, *95* (1), 176–184.
(11) Myers, C. R.; Nealson, K. H. Bacterial manganese reduction and growth with manganese oxide as the sole electron acceptor. *Science* **1988**, *240* (4857), 1319–1321.
(12) Venkateswaran, K.; Moser, D.; Dollhopf, M.; Lies, D.; Saffarini, D.; MacGregor, B.; Ringelberg, D.; White, D.; Nishijima, M.; Sano, H. Polyphasic taxonomy of the genus Shewanella and description of Shewanella oneidensis sp. *Int. J. Syst. Bacteriol.* **1999**, *49* (2), 705–724.
(13) Tang, Y. J.; Meadows, A. L.; Keasling, J. D. A kinetic model describing Shewanella oneidensis MR-1 growth, substrate consumption, and product secretion. *Biotechnol. Bioeng.* **2007**, *96* (1), 125–133.
(14) Tang, Y. J.; Meadows, A. L.; Kirby, J.; Keasling, J. D. Anaerobic central metabolic pathways in Shewanella oneidensis MR-1 reinterpreted in the light of isotopic metabolite Labeling. *J. Bacteriol.* **2007**, *189* (3), 894–901.
(15) Mitchell, A. C.; Phillips, A. J.; Hamilton, M. A.; Gerlach, R.; Hollis, W. K.; Kaszuba, J. P.; Cunningham, A. B. Resilience of planktonic and biofim culutres to supercritical CO_2. *J. Supercrit. Fluids* **2008**, *47*, 318–325.
(16) Mitchell, A. C.; Phillips, A. J.; Hiebert, R.; Gerlach, R.; Spangler, L. H.; Cunningham, A. B. Biofilm enhanced geologic sequestration of supercritical CO_2. *Int. J. Greenhouse Gas Control* **2009**, *3*, 90–99.
(17) Mitchell, A. C.; Dideriksen, K.; Spangler, L. H.; Cunningham, A. B.; Gerlach, R. Microbially enhanced carbon capture and storage by mineral-trapping and solubility-trapping. *Environ. Sci. Technol.* **2010**, *44* (13), 5270–5276.
(18) Stumm, W.; Morgan, J. J. *Aquatic Chemistry: Chemical Equilibria and Rates in Natural Waters*; John Wiley & Sons: New York, 1996.
(19) Shao, H.; Ray, J. R.; Jun, Y.-S. Dissolution and Precipitation of Clay Minerals under Geologic CO_2 Sequestration Conditions: CO_2-Brine-Phlogopite Interactions. *Environ. Sci. Technol.* **2010**, *44* (15), 5999–6005.
(20) White, C. M.; Straziser, B. R.; Granite, E. J.; Hoffman, J. S.; Pennline, H. W. Separation and capture of CO_2 from large stationary sources and sequestration in geological formations-coalbeds and deep saline aquifers. *J. Air Waste Manage. Assoc.* **2003**, *53*, 645–715.
(21) Wu, B. *Enhanced membrane bioreactor by optimization of bacterial population*. Ph.D. thesis,Nanyang Technological University, Singapore, 2007.
(22) Dubois, M.; Gilles, K. A.; Hamilton, J. K.; Rebers, P. A.; Smith, F. Colorimetric Method for Determination of Sugars and Related Substances. *Anal. Chem.* **1956**, *28*, 350–356.
(23) Bradford, M. M. Rapid and Sensitive Method for the Quantitation of Microgram Quantities of Protein Utilizing the Principle of Protein-dye Binding. *Anal. Biochem.* **1976**, *72*, 248–254.
(24) Wu, B.; An, Y. Y.; Li, Y. Z.; Wong, F. S. Effect of adsorption/coagulation on membrane fouling in microfiltration process post-treating anaerobic digestion effluent. *Desalination* **2009**, *242* (1−3), 183–192.
(25) Hong, S. I.; Pyun, Y. R. Inactivation kinetics of Lactobacillus plantarum by high pressure carbon dioxide. *J. Food Sci.* **1999**, *64* (4), 728–733.
(26) Oule, M. K.; Tano, K.; Bernier, A.-M. Arul, J. Escherichia coli inactivation mechanism by pressurized CO_2. *Can. J. Microbiol.* **2006**, *52*, 1208–1217.
(27) Ulmer, H. M.; Ganzle, M. G.; Vogel, R. F. Effects of high pressure on survival and metabolic activity of Lactobacillus plantarum TMW1.460. *Appl. Environ. Microbiol.* **2000**, *66* (9), 3966–3973.
(28) Knox, P. R.; Paine, J. G.; Hovorka, S. D. Optimal Geological Environments for Carbon Dioxide Disposal in Brine Formations (Saline Aquifers) in the United States—Pilot Experiment in the Frio Formation, Houston Area: Contract DE-AC26-98FT40417 Modification A008, 2003.
(29) Leaphart, A. B.; Thompson, D. K.; Huang, K.; Alm, E.; Wan, X. F.; Arkin, A.; Brown, S. D.; Wu, L. Y.; Yan, T. F.; Liu, X. D.; Wickham, G. S.; Zhou, J. Z. Transcriptome profiling of Shewanella oneidensis gene expression following exposure to acidic and alkaline pH. *J. Bacteriol.* **2006**, *188* (4), 1633–1642.

ES102299J